

# Geochemistry and petrogenesis of anorogenic basic volcanic-plutonic rocks of the Kundal area, Malani Igneous Suite, western Rajasthan, India

A KRISHNAKANTA SINGH\* and G VALLINAYAGAM\*\*

\*Wadia Institute of Himalayan Geology, Northeast Unit, Vivek Vihar, Itanagar 791 113, India.

\*\*Department of Earth Sciences, Kurukshetra University, Kurukshetra 136 119, India.

\*e-mail: kk\_luwang@rediffmail.com

The Kundal area of Malani Igneous Suite consists of volcano-plutonic rocks. Basalt flows and gabbro intrusives are associated with rhyolite. Both the basic rocks consist of similar mineralogy of plagioclase, clinopyroxene as essential and Fe-Ti oxides as accessories. Basalt displays sub-ophitic and glomeroporphyritic textures whereas gabbro exhibits sub-ophitic, porphyritic and intergranular textures. They show comparable chemistry and are enriched in Fe, Ti and incompatible elements as compared to MORB/CFB. Samples are enriched in LREE and slightly depleted HREE patterns with least significant positive Eu anomalies. Petrographical study and petrogenetic modeling of [Mg]-[Fe], trace and REE suggest cogenetic origin of these basic rocks and they probably derived from Fe-enriched source with higher Fe/Mg ratio than primitive mantle source. Thus, it is concluded that the basic volcano-plutonic rocks of Kundal area are the result of a low to moderate degree (< 30%) partial melting of source similar to picrite/komatiitic composition. Within plate, anorogenic setting for the basic rocks of Kundal area is suggested, which is in conformity with the similar setting for Malani Igneous Suite.

## 1. Introduction

The Malani magmatism is characterized by sub-volcanic setting, volcano-plutonic ring structures, anorogenic (A-type), high heat producing magmatism and controlled by NE-SW trending lineaments and is related to hot-spot activity (Kochhar 1984; Kochhar 1989; Vallinayagam and Kochhar 1998; Bhushan and Chittora 1999). The Malani Igneous Suite (MIS) covers an area about 55,000 sq km in the trans-Aravalli block of Rajasthan and Haryana, with a possible extension to Sind Province in Pakistan (Bhushan and Chittora 1999; Kochhar 2000). The volcano-plutonic association of MIS has three stages of igneous activity (Bhushan 1984). The bimodal evolved through basic and acid volcanic flows represent the first phase. This was followed by a major plutonic activity of plutons, bosses and

ring dykes of granites. The third phase includes acid and basic dykes. Preponderance of acid volcanics over intermediate and basic volcanic is a distinctive feature of MIS. The isotopic data (Rb/Sr age) reveals the Neoproterozoic age ( $725 \pm 7$  Ma) for the MIS (Dhar *et al* 1996). Recently, Torsvik *et al* (2001) reported U-Pb ages of Malani rhyolite between 771 and 751 Ma. Limited published work is available on the basic rocks of MIS. However, a very comprehensive account on the petrography and geochemistry of basic rocks from MIS has been reported by few workers (Kochhar *et al* 1995; Vallinayagam 1997; Vallinayagam and Kochhar 1998; Bhushan and Chittora 1999; Vallinayagam 2001).

The Kundal area of MIS is characterized by A-type granites with carapace of cogenetic acid volcanics (rhyolite, trachyte, welded tuff) with

**Keywords.** Petrogenesis; basalt; gabbro; Kundal; Malani Igneous Suite.

minor amount of basalt, gabbro, dolerite (Singh and Vallinayagam 2002). The geological mapping reveals a close association of acid volcanics with the granites and basic volcanics with gabbros, indicating interrelationship between volcanism and plutonism. However, no detailed geochemical studies of Kundal basic rocks are available. Hence, the present paper attempts to discuss the petrogenesis and tectonic setting of these rocks based on geochemical studies.

## 2. Geological setting and petrography

Based on detailed geological mapping (figure 1b) and field studies around Kundal, the rock units encountered in the area can be grouped as:

- Extrusive phase: basalt, trachyte, rhyolite with minor amount of welded tuffs;
- Intrusive phase: gabbro, granite and
- Dyke phase: dolerite (younger).

Flows of basalt are intercalated with porphyritic rhyolite whereas gabbro occurs as small intrusive within non-porphyritic and porphyritic rhyolites. Occasionally basalt displays vesicular and amygdaloidal structures. Numerous calcite veins (length 0.5 to 6 m and width 1.5 to 15 cm) cut across basalt flow. The trachyte flow associated with rhyolite and volcanic ash bed (~ 100 m length and 5 m width) is exposed within the trachyte flow. Granites have intruded porphyritic rhyolite with sharp contact and marked by distinct morphological change. They show encrustations of iron oxide and growth of pegmatite. Two types of gabbro are identified in the field i.e., dark green medium grained (gabbro I) and dark green coarse grained (gabbro II). Gabbro I consists of radiating laths of plagioclase feldspar in the groundmass of dark green clinopyroxene (augite) and iron oxides. Plagioclase feldspars in various shapes (lath, rectangular, rhombohedral and elliptical) and sizes (ranging length 6–12 cm and width 1–7 cm) are embedded in the ferromagnesian groundmass of gabbro II. Xenoliths of basalt are also encountered in the rhyolite and trachyte. The acid volcanic rocks are invariably cut across by numerous NE-SW, NW-SE trending dolerite dykes.

Both the basic rocks show similar mineralogy of plagioclase feldspar (labradorite), clinopyroxene (augite) as essential minerals and magnetite and ilmenite as accessory phases. Basalt displays subophitic and glomeroporphyritic textures. The gabbro I shows sub-ophitic texture whereas gabbro II shows porphyritic and intergranular textures. Labradorite ( $An_{55-60}$ ) occurs in euhedral to subhedral forms with corroded margins and faint clouding. At places, it is replaced by albite and is altered

to kaolin. Augite occurs as short prismatic crystals and shows two directional cleavage and the extinction angle ( $Z \wedge C$ ) varies between  $36^\circ$  and  $47^\circ$ . Some of the augite phenocrysts display exsolved blebs of labradorite. At places, labradorite and opaque are seen as embedded augite. Magnetite and ilmenite occurs as anhedral and small elongated, irregular, isotropic crystals in the ferromagnesian groundmass. The plagioclase feldspar is altered to sericite and only skeletal forms are seen in the ferromagnesian groundmass. At places, ilmenite is partly replaced by leucoxene and magnetite by hematite. In gabbro I calcite veins are developed within the groundmass. The groundmass consists of microcrystalline aggregates of labradorite, augite and Fe-Ti oxides. Xenoliths of basalt display similar textural and mineral characters of basalt flow. The plagioclase feldspar shows more intense alteration at the margin than in the core. It is altered to sericite and only skeletal forms are seen in the ferromagnesian groundmass.

## 3. Geochemistry

Major elements analyses were carried out at the Department of Earth Sciences, KU, Kurukshetra by using synchronic UV-VIS Spectrometer-108 and Mediflame Photometer-27. Trace elements including rare earth elements were analysed by ICP-AES at School of Environmental Sciences, JNU, New Delhi. The analytical precision is found to be in the error level  $< 5\%$  for major and  $< 10\%$  for trace elements. Major elements of Kundal basalt and gabbros are represented in table 1 and trace elements including REE concentrations of these rocks are given in table 2.

The  $SiO_2$  content of basalt is about 45.21 wt% on the average. It has high  $Fe_2O_3$  content ranging between 13.72 and 15.39 wt%.  $TiO_2$  shows high concentration (2.92 to 3.96 wt%), this is reflected by the presence of ilmenite in the samples.  $MgO$  varies from 5.75 to 6.81 wt%. The  $Mg \#$  varies from 42.53 to 48.05 and  $CaO$  from 6.23 to 7.92 wt%. Basalts are rich in total alkali oxides (4.90–5.45 wt%) and have high  $Na_2O/K_2O$  ratios ranging from 3.42 to 4.39 wt%. The  $NK/C$  and  $A/CNK$  ratios are 0.61 to 0.86 and 0.64 to 0.75 respectively. Gabbros show restricted range of  $SiO_2$  (51.12 to 56.52 wt%). The  $Fe_2O_3^{(t)}$  shows wide variation from 9.87 to 15.10 wt%. Plagioclase rich rock samples show low values of  $TiO_2$ . They are enriched  $Na_2O$  (4.42 to 5.71 wt%) as compared to  $K_2O$  (0.37 to 0.95 wt%).  $CaO$  and  $MgO$  varies from 3.85 to 5.10 wt% and 5.75 to 6.81 wt% respectively.  $Mg \#$  shows wide variation from 37.07 to 55.28. The  $NK/C$  and  $A/CNK$  show ranges of 1.01 to 1.68 and 0.84 to 0.94 respectively. Basalt shows high  $TiO_2$

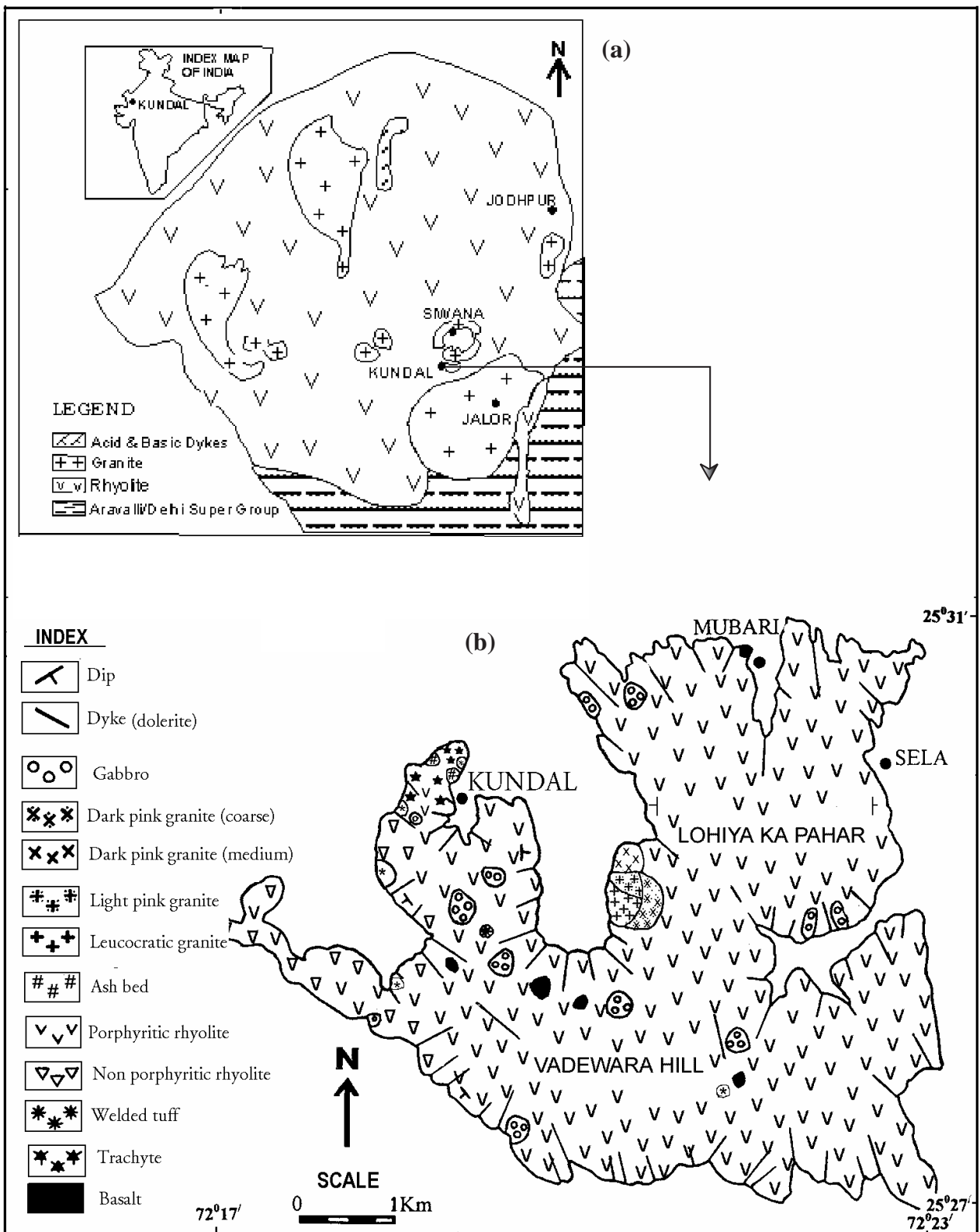


Figure 1. (a) Simplified geological map of Malani Igneous Suite, northwestern Indian Shield (modified after Bhushan 1985). (b) Geological map of Kundal area of Malani Igneous Suite.

(2.92 to 3.96 wt%) as compared to gabbro (1.17 to 2.72 wt%). Variation in  $TiO_2$  concentration in these rocks may be a result of fractionation (Sun

and Nesbitt 1977). In the TAS (total alkali-silica) diagram (Le Bas *et al* 1986), the basalt falls in the field of basalt. In the  $Na_2O + K_2O$  vs  $SiO_2$  diagram

Table 1. Major element analyses of the Kundal basalt and gabbro rocks, Malani Igneous Suite, western Rajasthan, India.

Rock type	Basalt						
Sample no.	BKB20	BKB21	BKB41	BKB46	BKN16	BKN42	BKN55
Oxide							
SiO <sub>2</sub>	44.92	45.00	45.51	44.02	46.21	44.86	46.00
TiO <sub>2</sub>	3.76	3.01	2.96	3.51	3.31	2.92	3.96
Al <sub>2</sub> O <sub>3</sub>	14.83	14.24	14.41	14.22	14.71	14.76	14.06
Fe <sub>2</sub> O <sub>3</sub> <sup>(t)</sup>	13.72	13.96	15.11	15.09	15.39	14.61	14.98
MnO	0.19	0.30	0.25	0.31	0.27	0.27	0.29
MgO	6.23	6.52	6.13	6.81	5.75	5.86	5.96
CaO	7.92	7.06	7.81	7.59	6.23	6.85	6.97
Na <sub>2</sub> O	3.87	4.44	4.01	3.88	4.15	4.26	4.21
K <sub>2</sub> O	1.03	1.01	0.95	1.02	1.21	1.17	1.08
P <sub>2</sub> O <sub>5</sub>	1.71	1.55	1.23	1.11	1.13	1.36	1.12
H <sub>2</sub> O	0.46	0.67	0.42	0.59	0.62	0.71	0.76
<b>Total</b>	<b>98.64</b>	<b>97.76</b>	<b>98.79</b>	<b>98.15</b>	<b>98.98</b>	<b>97.63</b>	<b>99.39</b>
CaO/Al <sub>2</sub> O <sub>3</sub>	0.53	0.49	0.54	0.53	0.42	0.46	0.49
Al <sub>2</sub> O <sub>3</sub> /TiO <sub>2</sub>	3.94	4.73	4.86	4.05	4.44	5.05	3.55
CaO/TiO <sub>2</sub>	2.10	2.34	2.63	2.16	1.88	2.34	1.76
Fe <sub>2</sub> O <sub>3</sub> /MgO	2.20	2.14	2.46	2.21	2.67	2.49	2.51
(Na <sub>2</sub> O + K <sub>2</sub> O)	4.90	5.45	4.96	4.90	5.36	5.43	5.36
(Na <sub>2</sub> O/K <sub>2</sub> O)	3.75	4.39	4.22	3.80	3.42	3.64	3.42
KN/C	0.61	0.77	0.63	0.64	0.86	0.79	0.75
A/CNK	0.68	0.64	0.65	0.67	0.75	0.71	0.67
An/An + Ab	0.37	0.29	0.35	0.35	0.33	0.32	0.31

Rock type	Gabbro I (medium)					Gabbro II (coarse)		
Sample no.	GKB19	GKB21	GKB40	GKN49	GVK32	GKB17	GKB38	GKB48
Oxide								
SiO <sub>2</sub>	51.12	52.31	55.16	53.32	52.56	56.52	56.32	55.92
TiO <sub>2</sub>	2.72	1.21	2.03	2.02	1.87	1.51	1.17	1.26
Al <sub>2</sub> O <sub>3</sub>	15.08	14.56	14.36	15.13	14.92	14.62	15.53	15.63
Fe <sub>2</sub> O <sub>3</sub> <sup>(t)</sup>	14.10	15.10	13.82	12.92	14.11	10.11	10.03	9.87
MnO	0.17	0.27	0.20	0.18	0.23	0.13	0.12	0.12
MgO	4.87	5.61	4.11	4.62	4.67	6.21	6.00	6.16
CaO	5.10	4.12	4.00	5.09	4.82	3.85	3.93	3.87
Na <sub>2</sub> O	4.42	4.47	4.76	4.72	4.52	5.22	5.63	5.71
K <sub>2</sub> O	0.74	0.72	0.37	0.72	0.37	0.95	0.87	0.82
P <sub>2</sub> O <sub>5</sub>	0.81	0.68	0.54	0.61	0.72	0.83	0.81	0.81
H <sub>2</sub> O	0.51	0.49	0.84	0.79	0.84	0.81	0.52	0.72
<b>Total</b>	<b>99.69</b>	<b>99.63</b>	<b>100.19</b>	<b>100.12</b>	<b>99.63</b>	<b>100.76</b>	<b>100.93</b>	<b>100.89</b>
CaO/Al <sub>2</sub> O <sub>3</sub>	0.33	0.28	0.27	0.33	0.32	0.26	0.25	0.24
Al <sub>2</sub> O <sub>3</sub> /TiO <sub>2</sub>	5.54	12.03	7.07	7.49	7.97	9.68	13.27	12.40
CaO/TiO <sub>2</sub>	1.87	3.40	1.97	2.51	2.57	2.54	3.35	3.07
Fe <sub>2</sub> O <sub>3</sub> /MgO	2.89	2.69	3.21	2.79	3.02	1.62	1.67	1.60
(Na <sub>2</sub> O + K <sub>2</sub> O)	5.16	5.19	5.13	5.44	4.89	6.17	6.50	6.53
(Na <sub>2</sub> O/K <sub>2</sub> O)	5.97	6.20	12.86	6.55	12.21	5.49	6.47	9.94
KN/C	1.01	1.25	1.28	1.06	1.01	1.60	1.65	1.68
A/CNK	0.86	0.94	0.93	0.88	0.90	0.88	0.89	0.90
An/An + Ab	0.33	0.29	0.28	0.31	0.33	0.23	0.23	0.22

(Kuno 1968) the basalt falls in the composition fields of alkali olivine basalt whereas gabbro plots in the field of high-alumina olivine basalt to olivine basalt field. All the analysed samples of basalt and gabbro I fall in the tholeiitic field whereas gabbro

II plot in the calc-alkaline field on SiO<sub>2</sub> vs Fe<sub>2</sub>O<sub>3</sub>/MgO diagram of Miyashiro (1974) (figure 2a). In the AFM diagram (Irvine and Baragar 1971), basalt and gabbro I show a transition from calc-alkaline to tholeiitic with moderate iron

Table 2. Trace element (including rare earth elements) data for Kundal basic rocks, Malani Igneous Suite, Rajasthan, India.

Rock type	Basalt			Gabbro I		Gabbro II
Sample no.	BKN16	BKB20	BKB41	GKB21	GKN49	GKB38
Cr	10	54	21	49	42	44
Ni	74	101	99	86	69	75
Ba	243	224	296	365	301	213
Sr	421	387	320	386	349	429
Rb	81	46	ND	47	ND	61
Nb	20	24	ND	16	ND	19
Zr	210	265	165	256	267	239
Y	30	67	48	42	47	46
Ratios						
Zr/Nb	10.5	11.04	----	6.09	----	12.57
Zr/Y	7.0	3.95	3.43	6.09	5.68	5.19
Y/Nb	1.5	2.79	----	2.62	----	2.42
Ti/Zr	94.4	85.06	107.5	28.33	45.35	29.34
Nb/Ti	0.001	0.001	----	0.002	----	0.002
Zr/Ti	0.01	0.01	0.009	0.03	0.02	0.03
REE						
Ce	36.67	39.37	ND	26.25	ND	28.80
Nd	26.02	27.64	ND	17.56	ND	19.41
Sm	6.11	7.33	ND	4.12	ND	5.16
Eu	2.62	2.94	ND	2.03	ND	2.11
Gd	8.37	9.21	ND	5.16	ND	6.42
Dy	6.54	7.85	ND	4.24	ND	5.38
Er	4.30	5.33	ND	2.79	ND	3.85
Yb	3.16	3.92	ND	2.01	ND	2.69
REE(t)	93.79	103.59	----	64.16	----	73.82
Ratios						
(Ce/Nd) <sub>N</sub>	1.03	1.05	----	1.08	----	1.09
(Sm/Nd) <sub>N</sub>	0.73	0.82	----	0.82	----	0.72
(Ce/Sm) <sub>N</sub>	1.41	1.26	----	1.31	----	1.50
(Gd/Yb) <sub>N</sub>	2.12	1.88	----	1.91	----	2.06
(Ce/Yb) <sub>N</sub>	2.96	2.57	----	2.73	----	3.34
Eu/Eu*	1.13	1.10	----	1.13	----	1.35

ND = not determined.

enrichment whereas gabbro II shows calc-alkaline with moderate alkali enrichment. When these rocks are plotted in  $\text{Al}_2\text{O}_3\text{-Fe}_2\text{O}_3^{(t)} + \text{TiO}_2\text{-MgO}$  diagram (Jensen 1976), basalt and gabbro I plot in high Fe-tholeiitic field whereas gabbro II plots in high Mg-tholeiitic field (figure 2b). The  $\text{TiO}_2$  values decrease with increase in  $\text{CaO/TiO}_2$  and  $\text{Al}_2\text{O}_3/\text{TiO}_2$  ratios from gabbro II to gabbro I and from gabbro I to basalt (table 1). As the degree of melting increases, the ratios of  $\text{CaO/TiO}_2$  and  $\text{Al}_2\text{O}_3/\text{TiO}_2$  also increases while the Al and Ca phases gradually decreases in the residue. Thus, gabbro II was probably derived by a higher degree of partial melting than gabbro I and basalt.

The chondrite normalized REE patterns of selected basalt and gabbro samples are given in figure 3(a). Both the basic rocks show simi-

lar REE patterns of moderate LREE enrichment and slightly depleted HREE patterns with minor positive Eu anomalies. In both the rock type fractionation is more in HREE as compared to LREE. Variation in Sm/Nd ratios can be attributed to different extents of partial melting (Balakrishnan 1986). The  $(\text{Ce/Sm})_N$  ratios (1.31–2.26) are almost the same as  $(\text{Gd/Yb})_N$  ratios (1.88–2.16). Thus, enrichment from HREE to LREE is generally uniform and regular.  $\text{Eu/Eu}^*$  shows narrow variation in both the rock types, ranging from 1.10 to 1.35. There is a decrease in  $\text{Eu/Eu}^*$  with increasing REE concentrations. The REE patterns of these rocks are sub-parallel to one another. They exhibit relatively flat normalized patterns. The positive Eu anomalies may be due to melting of plagioclase bearing source or accumulation of plagioclase

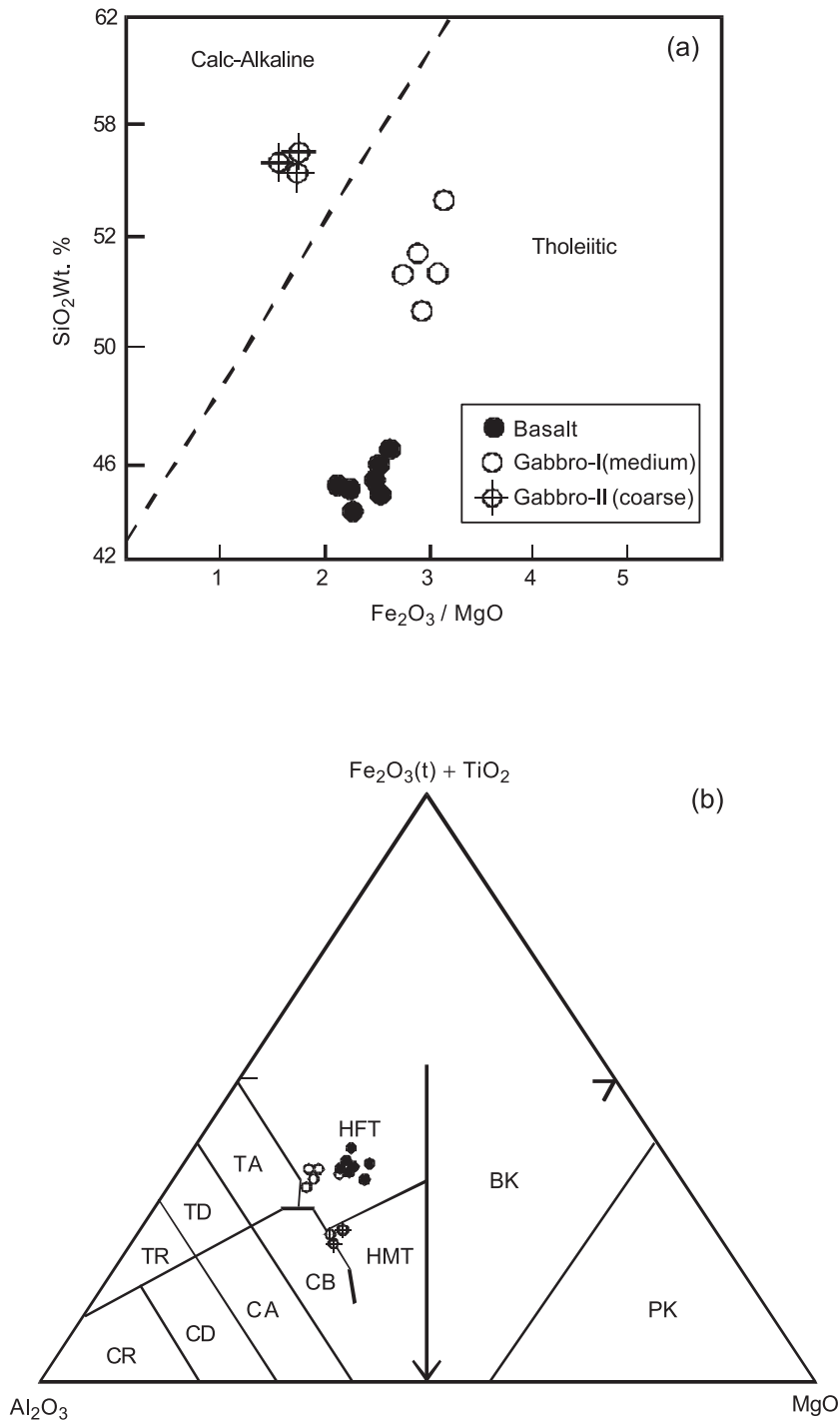


Figure 2. (a)  $\text{SiO}_2$ - $\text{Fe}_2\text{O}_3/\text{MgO}$  diagram (Miyashiro 1974). (b)  $\text{Al}_2\text{O}_3$ - $\text{Fe}_2\text{O}_3(t) + \text{TiO}_2$ - $\text{MgO}$  diagram (Jensen 1976) for the Kundal basalt and gabbros. **TA**: tholeiitic andesite, **TD**: tholeiitic dacite, **TR**: tholeiitic rhyolite, **CA**: calc-alkaline dacite, **CB**: calc-alkaline basalt, **CD**: calc-alkaline dacite, **CR**: calc-alkaline rhyolite, **BK**: basaltic komatiite, **PK**: peridotitic komatiite, **HFT**: high Fe-tholeiitic and **HMT**: high Mg-tholeiitic. Symbols: ● = basalt; ○ = gabbro I; ⊕ = gabbro II.

during fractionalization of parental liquid (Hanson 1980). The sub-parallel REE patterns indicate fractionation of REE in relatively constant proportions over a significant range of compositions. Primordial mantle normalized trace elements spider diagram (normalization values from Sun and McDonough 1989) for selected Kundal basalt and gabbros are

shown in figure 3(b). They are characterized by a general enrichment from less incompatible to more incompatible elements with negative Rb, K and P anomalies and general enrichment in large ion lithophile elements (LILE) and light rare earth element (LREE) which are characterized by many continental basalts (Storey *et al* 1992). Plagioclase

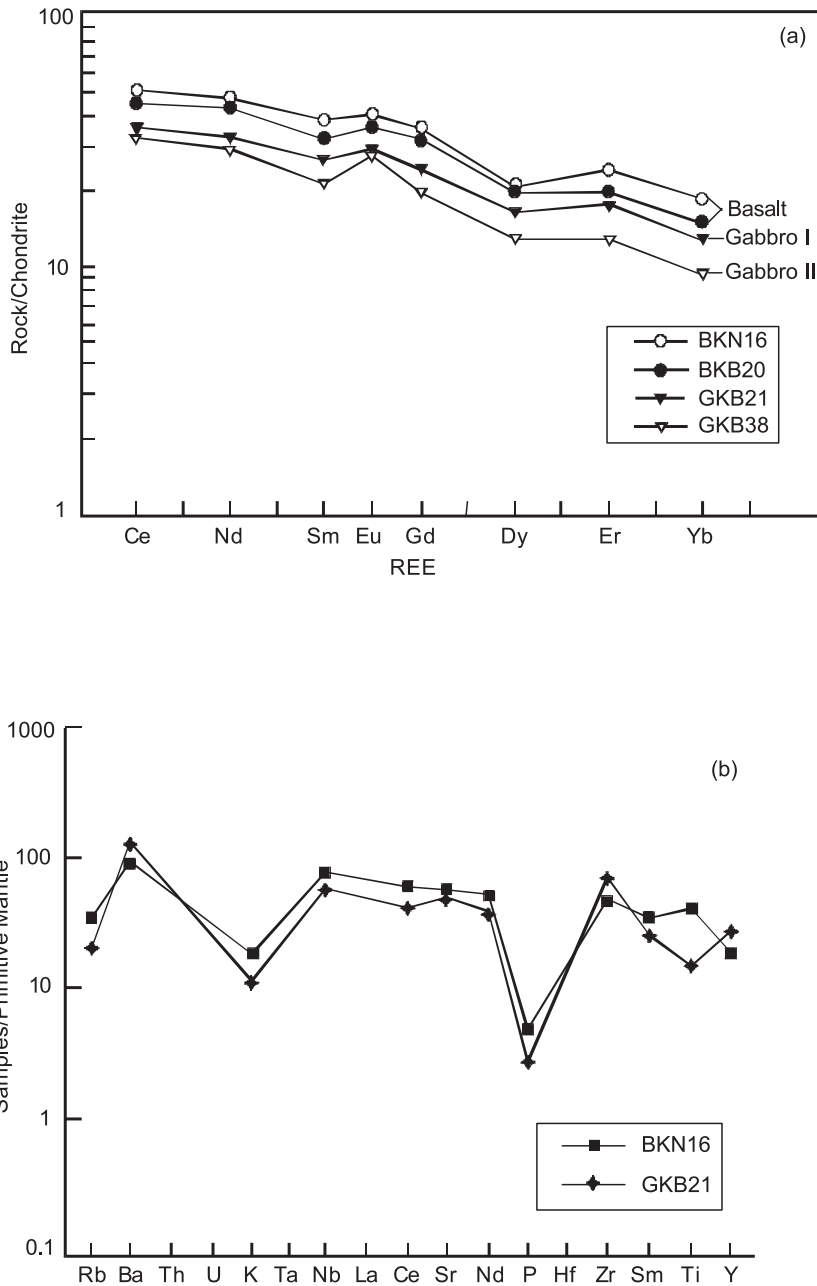


Figure 3. (a) Chondrite-normalized REE patterns of Kundal basalt and gabbro rocks (normalization factors from Masuda *et al* 1973). (b) Primitive-mantle normalized trace elements diagram for selected Kundal basalt and gabbro rocks (normalization values from Sun and McDonough 1989)

melting in the source region could be one reason for the Sr enrichment (Defant and Drummond 1990). Elements such as Ba, Nb, Zr show peaks and Rb, K show marked troughs.

#### 4. Petrogenesis and tectonic setting

##### 4.1 [Mg]-[Fe] modeling

The [Mg]-[Fe] modeling was initially proposed by Hanson and Langmuir (1978) and Langmuir and

Hanson (1980) to understand the physical conditions of magma generation, the nature of mantle sources and the extent of partial melting of basic rocks. It was subsequently modified by Rajamani *et al* (1993) as [Mg]-[Fe] diagram in the light of experimental data of Ford *et al* (1983).

The calculated [Mg]-[Fe] values, liquidus temperatures and other relevant petrogenetic parameters for the Kundal basic rocks are presented in table 3. The [Mg]-[Fe] values plot in the calculated melt fields on the [Mg]-[Fe] diagram (figure 4a) for theoretical melting of garnet-lherzolite with

Table 3. Petrogenetic parameters for the Kundal basic rocks, Malani Igneous Suite, Rajasthan, India.

Rock type	Gabbro I (medium)					Gabbro II (coarse)		
Sample no.	GKB19	GKB21	GKB40	GKN49	GVK32	GKB17	GKB38	GVK48
[Mg]%	14.14	15.53	13.20	14.31	13.74	20.22	20.04	20.54
[Fe]%	17.75	19.17	19.72	17.31	18.50	14.45	14.43	14.12
Kd <sub>Mg</sub>	6.07	5.38	6.72	6.53	6.14	5.94	6.19	6.10
Kd <sub>Fe</sub>	2.42	2.20	2.75	2.60	2.52	2.24	2.30	2.24
KDX	0.40	0.41	0.41	0.40	0.41	0.38	0.37	0.37
Fo-ol	63.15	64.27	59.00	63.99	61.48	76.33	76.16	77.08
T°liqC	1319	1357	1319	1319	1318	1405	1402	1408
Mg#	40.62	41.46	42.39	37.07	39.59	54.23	54.88	55.28
Rock type	Basalt							
Sample no.	BKB20	BKB21	BKB41	BKB46	BKN16	BKN42	BKN55	—
[Mg]%	15.91	16.99	15.42	16.82	15.13	15.57	15.49	—
[Fe]%	14.35	15.06	15.83	15.33	16.97	16.04	16.03	—
Kd <sub>Mg</sub>	5.25	5.05	5.14	4.79	5.32	5.32	5.28	—
Kd <sub>Fe</sub>	1.97	1.88	1.96	1.77	2.03	2.00	1.98	—
KDX	0.38	0.37	0.38	0.37	0.38	0.38	0.38	—
Fo-ol	67.85	71.34	67.83	70.74	65.95	67.85	67.71	—
T°liqC	1331	1350	1327	1349	1331	1331	1330	—
Mg#	47.35	48.05	44.55	47.19	42.53	44.27	44.07	—

[Mg] and [Fe] = Compositionally corrected Mg and Fe abundances in cation mole per cent using Ford *et al* (1983) equation -3 based on compositionally corrected olivine-melt  $K_{dS}$ ' for MgO and FeO.

Kd<sub>Mg</sub> = Concentration of Mg in olivine/concentration of Mg in liquid.

Kd<sub>Fe</sub> = Concentration of Fe olivine/concentration of Fe in liquid.

KDX =  $K_{dFe}/K_{dMg}$ .

Fo-ol = Forsterite content of olivine with which liquid in equilibrium.

T°liqC = One atmosphere (0.001 kb) liquid olivine temperature calculated using equation -3 of Ford *et al* (1983).

Mg# =  $Mg/(Mg + Fe^t)$  cation mole per cent.

MgO = 37.9 and FeO = 10.2 at 0, 3 (~ 100 km depth) and 5 Ga pressure (Rajamani *et al* 1993). The solidii for 0, 3 and 5 GPa pressures are based on the experimental work of Takahashi (1986). The Kundal basic rocks plot outside the melt field (figure 4a) suggesting that they are not generated from a garnet-lherzolite source. The rocks show a gentle decrease of [Mg] with a steep increase of [Fe], thus the trend implies that the rocks related to one another by extent of melting of the source or fractional crystallization of olivine, plagioclase and clinopyroxene result in a trend sub-parallel to [Fe] axis (Rajamani *et al* 1989). The most primitive samples (gabbro II) plot to the right of the solidus. Even if we assume that they had undergone 20% olivine fractional crystallization, their parental magma would still plot to the right of the solidus. Hence, the source rock of the Kundal basic rocks magma had a much higher Fe/Mg ratio relative to garnet-lherzolite/pyrolite source (Rajamani *et al* 1989; Ahmad and Tarney 1994).

The lithospheric sources have a higher Fe/Mg ratio than that of pyrolite or lherzolite as a result of addition of melts generated at deeper levels (Ahmad and Rajamani 1991). The Komati-

itic amphibolites reported from Kolar Schist Belt (Rajamani *et al* 1985) have higher Fe/Mg ratio than garnet-lherzolite. Melt fields for a komatiitic source having 29.21 mole % MgO and 8.47 mole % FeO for 1 atmosphere and 25 kb pressures are shown in figure 4(b). The basalt and gabbro I samples plot below the solidus whereas the gabbro II samples plot inside the melt field suggesting that they represent primary melt composition. The gabbro II have high Mg (54.23–55.28) and liquidus olivine temperature (1402°C–1408°C) as compared to basalt and gabbro I which show low Mg # (37.07–47.35) and liquidus olivine temperature (1318°C–1357°C). There is an increase of [Fe] from gabbro II to basalt and gabbro I because fractionation of olivine above 1300°C increases the residual melt in Fe (Hanson and Langmuir 1978). The distribution coefficient of Mg in olivine relative to liquid  $K_d Mg^{01/1}$  decreases systematically with the increase of liquidus olivine temperature from gabbro II to basalt and gabbro I are related to one another by different extent of melting of the source. The samples show a negative correlation with Fe enrichment, suggesting that the crustal contamination may not have been

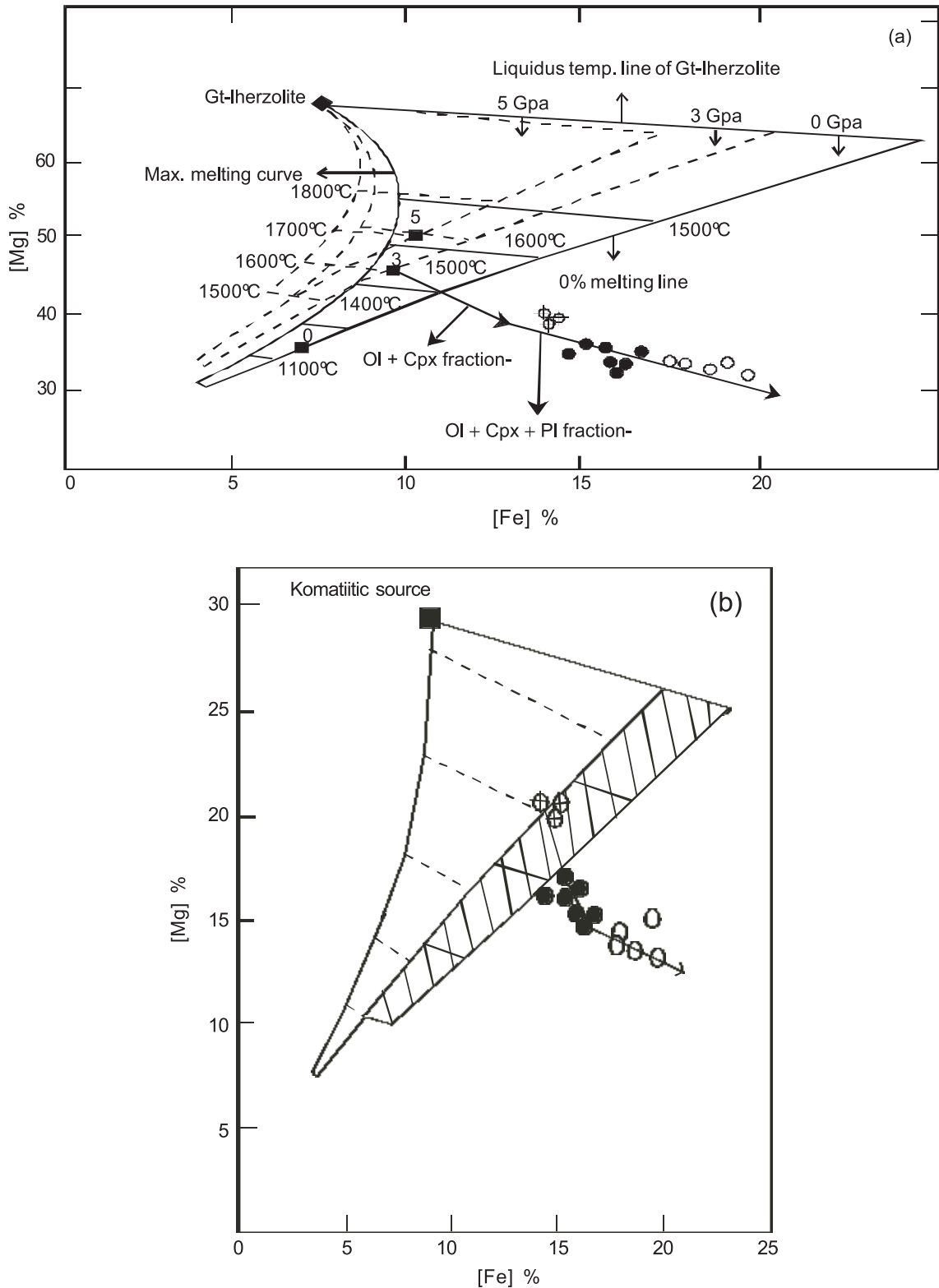


Figure 4. (a) Plot of Kundal basalt and gabbro rocks in the calculated [Mg]-[Fe] diagram (after Rajamani *et al* 1993). The diagram shows that melt field for batch melting of garnet-lherzolite at 0, 3 and 5 Gpa pressure. (b) Plot of Kundal basic rocks in the calculated [Mg]-[Fe] diagram (after Rajamani *et al* 1985). The melt fields are constructed for a Komatiitic source (filled square) at 1 atmosphere and 25 kb.

significant. High contents of  $\text{Fe}_2\text{O}_3^{(t)}$  and  $\text{TiO}_2$  also suggest that these rocks have not undergone considerable crustal contaminations (Arndt and Jen-

ner 1986). The low  $\text{CaO}/\text{Al}_2\text{O}_3$  ratios (0.24–0.54) in the samples suggest that garnet was not involved during the generation on these magmas.

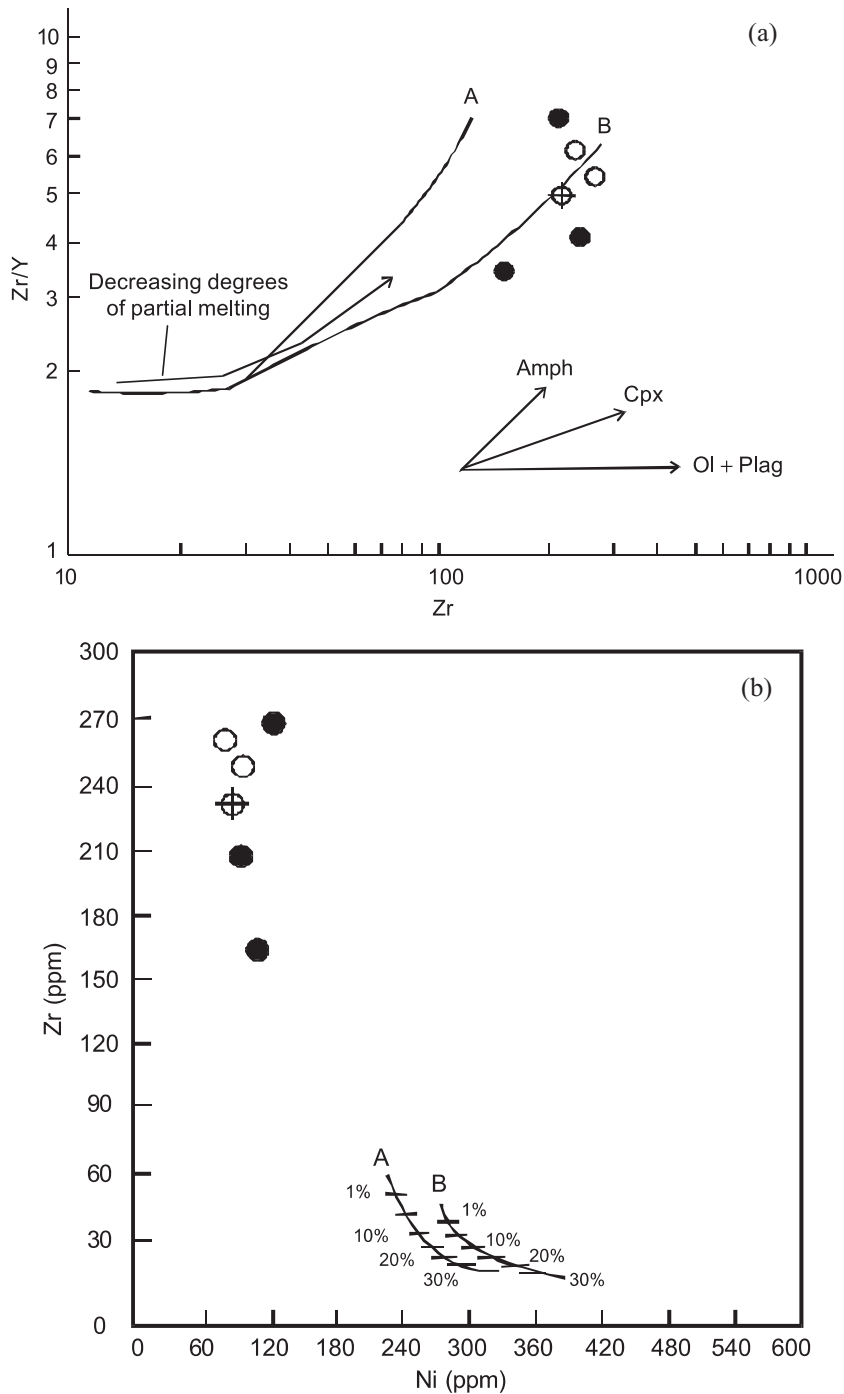


Figure 5. (a) Binary plot of Zr/Y vs. Zr for Kundal basic rocks. Melting curves A and B are after Drury (1983) and vectors for fractionation crystallization are after Floyd (1993) (b) Ni and Zr abundance in Ni vs. Zr plot after Rajamani *et al* (1985). Primitive mantle with 2000 ppm Ni and 8.3 ppm Zr is assumed as the source and two partial melting curves are constructed for two different residues: Curve A residuals mineralogy is 60% olivine and 40% pyroxene whereas 40% olivine and 60% pyroxene is assumed for curve B. The melt composition for 1, 5, 10, 15, 20, 25 and 30% batch melting of the mantle are indicated by the tick marks on both the curves. Note that the Kundal basic rock samples plot above 1% melt compositions. Therefore, their magma must have derived by partial melting of sources with higher Zr and lower Ni than the primitive mantle.

#### 4.2 Trace and REE modeling

The Kundal basic rocks have low Zr/Nb (6.07–12.57), Y/Nb (1.5–2.79), Ti/Zr (28.33–107.54) and high Zr/Y (3.43–7.00) ratio reflecting geochemi-

cal enriched nature of these basic rocks (Le Roex *et al* 1983). In binary plot of Zr/Y vs. Zr (figure 5a), samples show less variation in Zr/Y ratios with increasing of Zr abundances indicating olivine-plagioclase fractionation (Floyd 1993).

Two calculated partial melting curves (Drury 1983) (curve A: 60% olivine +20% opx +10% cpx +10% plagioclase; curve B: 60% olivine +20% opx +10% cpx +10% garnet) for Archaean mantle sources (Sun and Nesbitt 1977) are shown. The rock samples closely follow curve A indicating moderate to low degrees of partial melting of a garnet free mantle source, followed by clinopyroxene  $\pm$  olivine  $\pm$  plagioclase fractionation. In this diagram the analysed samples plot away from the crustal mantle mixing line however they display a trend that is close and parallel to enrichment trend suggesting that the enriched trace element characteristics of the Kundal basic rock is due to their generation from enriched mantle source relative to primitive mantle. In the Ni vs. Zr diagram (Rajamani *et al* 1985) (figure 5b), primitive mantle with 2000 ppm Ni and 8.3 ppm Zr is taken as the source (Taylor and McLennan 1985) and partial melting curves are constructed for two different residues as curve A and B. Residual mineralogy of curve A is 60% olivine and 40% pyroxene whereas 40% olivine and 60% pyroxene is assumed for curve B. These rock samples plot much above the calculated partial melting curves. Hence, the magma might have formed by partial melting of source with higher Zr and lower Ni than primitive mantle. Therefore, the primitive mantle is an unlikely source for their generation. The variable Zr abundances in the samples could have been predominantly as a result of different extents of partial melting.

The quantitative modeling of REE data of the basic rocks has been used to understand the nature of source rocks and the extent of partial melting and fractional crystallization process that their magma might have undergone. Major and trace element modeling reveal that the Kundal basic rock samples would have originated by partial melting of a source having higher abundances of compatible elements (Mg, Cr, Ni etc) than that of the basic rocks. A primitive mantle is considered as source rock that consists of 49.9 wt% SiO<sub>2</sub>, 35 wt% MgO, 8 wt% FeO, 2000 ppm Ni and 8.3 ppm Zr (Taylor and McLennan 1985). In the figure 6(a), chondrite normalized REE patterns of Kundal basic rocks (shaded zone) and calculated chondrite normalized REE patterns of different primitive mantle using batch melting equation:  $C_L/C_O = 1/D(1 - F) + F$  (Schilling 1966) are shown,  $K_d$  value used for calculations are those of Hanson (1980).  $P_1$  represents melt generated by 5% partial melting of the primitive mantle source leaving 40% olivine, 34% opx, 15% cpx and 11% plagioclase in the residue whereas  $P_2$  represents 10% partial melting of the same source leaving a residue comprised of 33% olivine, 45% opx and 19% cpx. The calculated melt  $P_1$  and  $P_2$  are plotted lower than the REE patterns of Kundal basic rocks. Hence, different

degrees of partial melting of the primitive mantle can not explain the various elemental abundances in these basic rock samples. It also suggests that the source of the basic rocks has lower Ni and higher Zr and REEs than the primitive mantle source. Again, we considered a picrite sample (no.1) from Nathdwara of Aravalli supergroup (Ahmad and Rajamani 1991) as source rock. This picrite source has 46.87 wt% SiO<sub>2</sub>, 7.70 wt% FeO<sup>(t)</sup>, 20.80 wt% MgO, 1090 ppm Ni. It shows moderate LREE with negative Eu anomaly. The calculated melting at 30% partial melting of the source leaving a residue consisting of 33% olivine, 48% opx and 19% cpx that broadly coincides with REE patterns of Kundal basic rock except Eu anomaly. The negative Eu anomaly in the source rock may be real or would be attributed to alterations as Eu, among the REE, is shown to be mobile (Jahn and Sun 1977). Hence, we considered a komatiitic amphibolite sample (no. SB 27-2) from Kolar Schist Belt (Balakrishnan 1986) as a source of Kundal basic rocks. This source has 47.80% SiO<sub>2</sub>, 11.02% FeO, 24.47% MgO, 1490 ppm Ni and 36 ppm Zr and the normative mineralogy is 33% olivine and 67% pyroxene. It shows LREE enriched chondrite normalized with the marked positive Eu anomaly REE pattern. Figure 6(b) shows chondrite normalized REE patterns for partial melts derived from the source and zone for the REE concentrations of basic rocks.  $S_1$  and  $S_2$  represent REE patterns of source derived by 15% and 25% partial melting leaving a similar residue used in partial melting of picrite source. The calculated melt ( $S_1$ ) at 15% partial melting closely approaches the higher REE abundances of the Kundal basalt whereas the calculated melt ( $S_2$ ) at 25% partial melting closely approaches the lower REE abundances of the Kundal gabbro. The similarity of REE patterns of the basic samples to the calculated REE patterns for 15% and 25% partial melting suggests that the REE abundances of the basic rock samples are possibly derived from the komatiitic amphibolite source. Hence, the Kundal basalt and gabbro could have been derived by different degrees of partial melting of source rock similar to komatiitic amphibolites/picritic composition.

### 4.3 Tectonic setting

The geochemical signatures of igneous suites often suggest tectonic setting prevailing at the time of emplacement. A number of tectonomagmatic discrimination diagrams have been used and the most commonly used discriminants are K<sub>2</sub>O, P<sub>2</sub>O<sub>5</sub>, MgO, Al<sub>2</sub>O<sub>3</sub>, FeO, Ti, Sr, Y and Zr. It is also a common practice to compare the trace and minor elements from known and unknown tectonic environments using spidergrams. However,

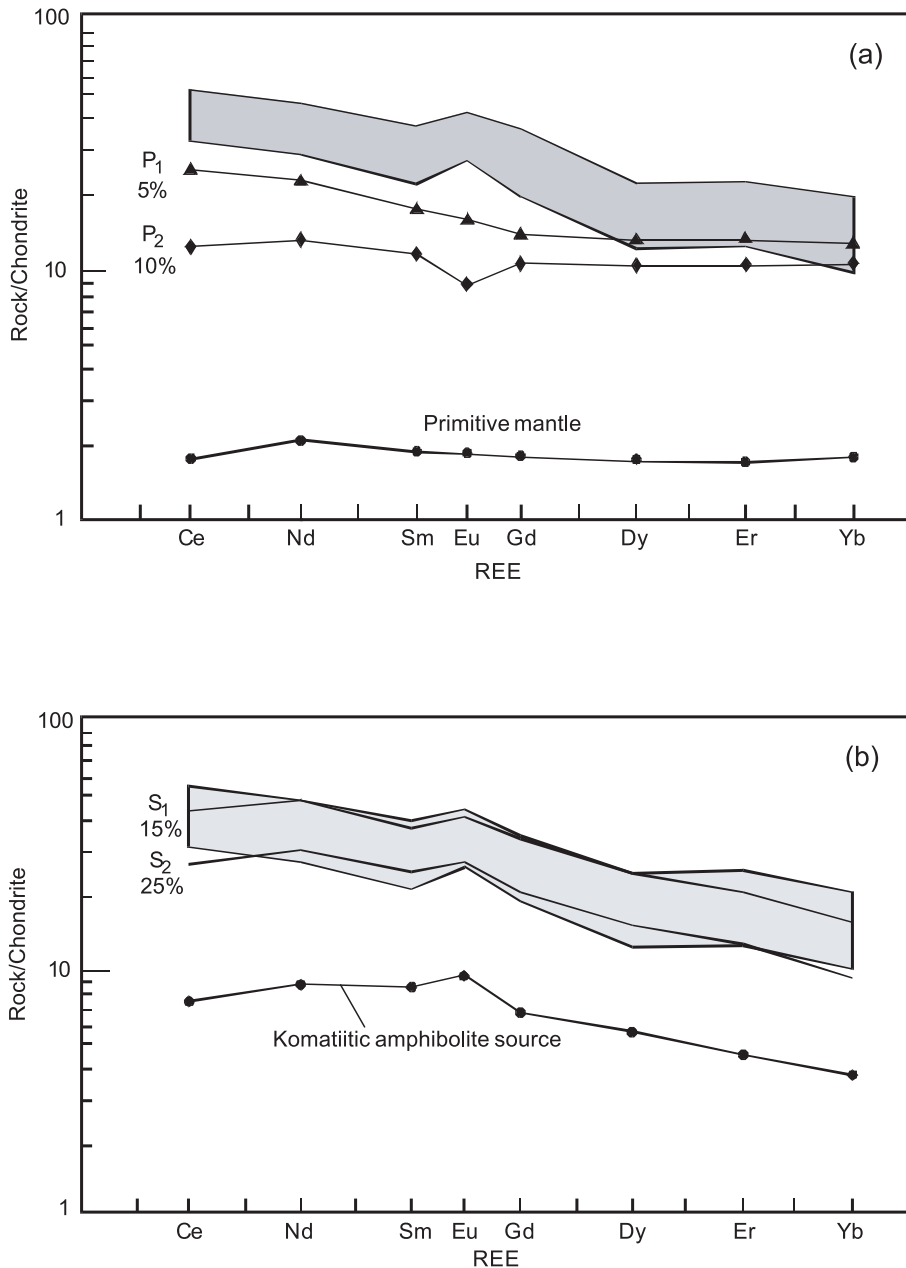


Figure 6. (a) Chondrite normalized plot for the partial melts of primitive mantle source.  $P_1$  represents the REE patterns of mantle leaving a residue consisting of 40% olivine, 34% opx, 15% cpx and 11% plagioclase on 10% partial melting.  $P_2$  represents melt leaving a residue 45% opx, 33% olivine 19% cpx on 5% partial melting of mantle. Note the Kunal basalt and gabbro samples (shaded zone) have higher REE abundances than the 5% mantle melts. (b) Chondrite normalized plot for komatiitic amphibolite source and calculated patterns for partial melts derived from these sources.  $S_1$  and  $S_2$  represent REE patterns of magma derived by 15% and 25% partial melting of the komatiitic amphibolite source leaving a residue consisting of 33% olivine, 48% cpx and 19% cpx. The REE abundances of the Kunal basic samples (shaded zone) are comparable to that of magma derived from the source.

some of the geochemical discriminant diagrams also show erroneous results (Duncan 1987). Thus, utmost care is needed to interpret the tectonic environment based upon these discriminants. As evidenced by the occurrence of basalt and gabbro, the rocks of Kunal area are being ponded by the basaltic magma in the region. In the tectonic discrimination diagram of the  $\text{TiO}_2\text{-K}_2\text{O-}$

$\text{P}_2\text{O}_5$  plot of Pearce *et al* (1975) (figure 7a) these rocks occupy the continental basalt field. These samples plot in the field of within plate basalt on the  $\text{TiO}_2$  vs Zr plot (Pearce 1980; figure 7b) and Cr-Y plot (Pearce 1982; figure 7c). The data support the anorogenic setting for the Malani Igneous rocks of the Trans-Aravalli block of the Indian shield.

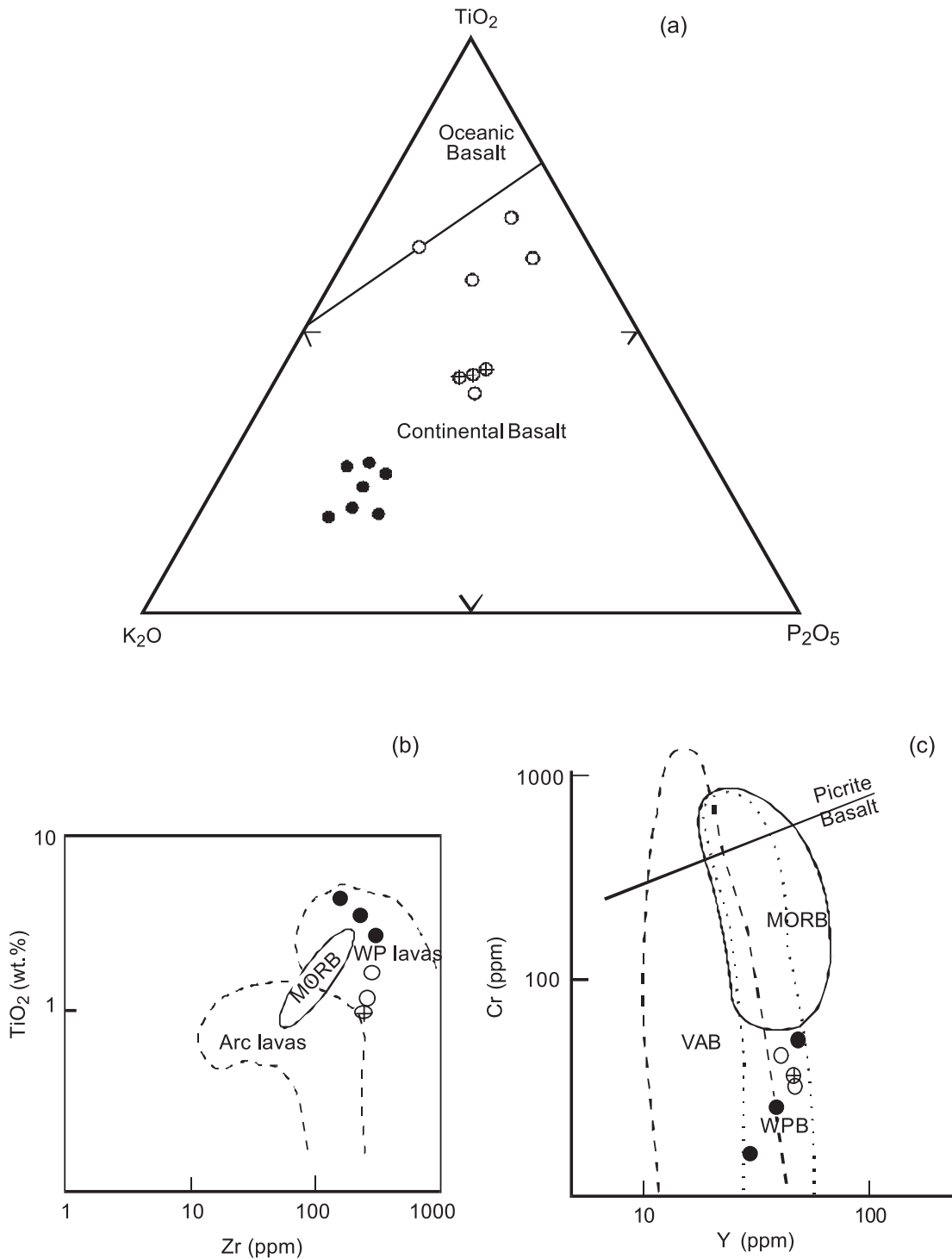


Figure 7. Tectonic discrimination diagrams of Kundal basic rocks (a)  $\text{TiO}_2$ - $\text{K}_2\text{O}$ - $\text{P}_2\text{O}_5$  plot (Pearce *et al* 1975) (b) Zr vs  $\text{TiO}_2$  plot (Pearce 1980) (c) Cr vs Y plot (Pearce 1982). **MORB**: mid oceanic ridge basalt; **WPB**: within plate basalt; **VAB**: volcanic arc basalt.

### Acknowledgements

The authors are grateful to Prof. V Rajamani, School of Environmental Sciences, JNU, New Delhi for providing laboratory facility for chemical analysis and fruitful discussion. We thank the reviewers, Prof. N Kochhar (Panjab

University) and Dr. M K Pandit (University of Rajasthan), for constructive and thoughtful reviews that significantly improved the content of the paper. A K Singh is thankful to the Director, Wadia Institute of Himalayan Geology, Dehradun, for permission to publish the present paper.

## References

- Ahmad T and Rajamani V 1991 Geochemistry and petrogenesis of the basal Aravalli volcanics near Nathdwara, Rajasthan, India; *Precam. Res.* **49** 185–204
- Ahmad T and Tarney J 1994 Geochemistry and petrogenesis of late Archaean Aravalli volcanics, basement enclaves and granitoids, Rajasthan; *Precam. Res.* **65** 1–23
- Arndt N T and Jenner G A 1986 Crustally contaminated komatiites and basalts from Kambalda, Western Australia; *Chem. Geol.* **56** 229–255
- Balakrishnan S 1986 Geochemical and isotopic studies of the amphibolites from the Kolar Schist Belt; *Unpublished Ph.D. thesis, Jawaharlal Nehru University, New Delhi* 237
- Bhushan S K 1984 Classification of Malani Igneous Suite; Symposium on three decades of developments in Petrology, Mineralogy and Petrochemistry in India; *Geol. Surv. Ind. Sp. Pub.* **12** 199–205
- Bhushan S K 1985 Malani volcanism in western Rajasthan, India; *J. Earth Sci.* **12**(1) 58–71
- Bhushan S K and Chittora V K 1999 Late Proterozoic bimodal volcanic assemblage of Siwana subsidence structure, western Rajasthan, India; *J. Geol. Soc. India* **53** 433–453
- Defant M J and Drummond M S 1990 Derivation of some modern arc magmas by melting of young subducted lithosphere; *Nature* **347** 662–665
- Dhar S, Frei R, Kramers J D, Nagler T F and Kochhar N 1996 Sr, Pb and Nd isotopes studies and their bearing on the petrogenesis of the Jalor and Siwana complexes, Rajasthan, India; *J. Geol. Soc. India* **48** 151–160
- Drury S A 1983 The petrogenesis and tectonic setting of Archaean metavolcanics from Karnataka state, south India; *Geochim. Cosmochim. Acta.* **47** 317–329
- Duncan A R 1987 The Karoo Igneous Province – a problem area for inferring tectonic setting from basalt geochemistry; *J. Volcano. Geotherm. Res.* **32** 13–34
- Floyd P A 1993 Geochemical discrimination and petrogenesis of alkaline basalt sequences in part of the Ankara mélangé, Central Turkey; *J. Geol. Soc. London* **150** 541–550
- Ford C E, Russell D G, Craven J A and Fisk M R 1983 Olivine-liquid equilibria: temperature, pressure and composition dependence of the crystal/liquid partition coefficient for Mg, Fe<sup>2+</sup>, Ca and Mn; *J. Petrol.* **24** 256–265
- Hanson G N 1980 Rare earth elements in petrogenetic studies of igneous rocks; *Ann. Rev. Earth Planet. Sci.* **8** 371–406
- Hanson G N and Langmuir C H 1978 Modeling of major element in mantle melt system using trace element approaches; *Geochim. Cosmochim. Acta.* **42** 725–741
- Irvine T N and Baragar W R A 1971 A guide to the chemical classification of the common volcanic rocks; *Can. J. Earth Sci.* **8** 523–548
- Jahn B M and Sun S S 1977 Trace element distribution and isotopic composition of Archaean greenstones. In: *Origin and distribution of the elements* (ed) L H Ahrens; *Physics and Chemistry of Earth*, (Oxford: Pergamon) 579–618
- Jensen L S 1976 A new cation plot for classifying sub-alkaline volcanic rocks; *Misc. Pap. Ontario, Div. Mines* No. **66**
- Kochhar N 1984 Malani Igneous Suite: hot-spot magmatism and cratonization of the northern part of Indian Shield; *J. Geol. Soc. India* **25**(2) 155–161
- Kochhar N 1989 High heat producing granites of the Malani Igneous Suite, northern Peninsular India; *Ind. Minerals* **43** 339–346
- Kochhar N 2000 Attributes and significance of the A-type Malani magmatism, north western Peninsular India. In: *Crustal evolution and metallogeny in the north western Indian shield* (ed) M Deb; (New Delhi: Narosa Publ.) 158–188
- Kochhar N, Dhar S and Sharma R 1995 Geochemistry and tectonic significance of acid and basic dykes associated with Jalor magmatism, west Rajasthan; *Mem. Geol. Soc. India* **33** 375–389
- Kuno H 1968 Differentiation of basalt magma from basalts. In: *The Poldervaart Treatise on rocks of basaltic compositions* (ed) H H Hess; (New York: Inter Science Publ.) 623–688
- Langmuir C H and Hanson G N 1980 An evaluation of major element heterogeneity in the mantle sources of basalts; *Philos. Trans. Royal Soc. London* **A297** 383–407
- Le Bas M J, Le Maitre R W, Streckeisen A and Zanethin B 1986 A chemical classification of volcanic rocks based on the total alkali-silica diagram; *J. Petrol.* **27** 745–750
- Le Roex A P, Dick H J B, Erlank A J, Reid A M, Frey F A and Hart S R 1983 Geochemistry, mineralogy and petrogenesis of lavas erupted along the south west Indian ridge between the Bouvet triple junction and 11 degrees east; *J. Petrol.* **24** 267–318
- Masuda A, Nakamura N and Tanaka T 1973 Fine structures of mutually normalized rare earth patterns of chondrites; *Geochim. Cosmochim. Acta.* **37** 239–248
- Miyashiro A 1974 Volcanic rock series in island arcs and active continental margins; *Amer. J. Sci.* **274** 321–355
- Pearce J A 1980 Geochemical evidence for the genesis and the eruptive setting of lavas from Tethyan ophiolites. In: *Ophiolites* (ed) A Panayiotou; *Proc. International Ophiolite Symposium, Nicosia, Cyprus* 261–272
- Pearce J A 1982 Statistical analysis of major element patterns in basalts; *J. Petrol.* **17** 15–43
- Pearce T H, Gorman B E and Birkett T C 1975 The TiO<sub>2</sub>-K<sub>2</sub>O-P<sub>2</sub>O<sub>5</sub> diagram: a method of discriminating between oceanic and non-oceanic basalts; *Earth Planet. Sci. Lett.* **24** 418–424
- Rajamani V, Balakrishnan S and Hanson G N 1993 Komatiite genesis: insights provided by Mg-Fe exchange equilibria; *J. Geol.* **101** 809–819
- Rajamani V, Shirey S B and Hanson G N 1989 Fe-rich Archaean tholeiites derived from melt enriched mantle sources: evidence from the Kolar Schist Belt, South India; *J. Geology* **97** 487–501
- Rajamani V, Shivkumar K, Hanson G N and Shirey S B 1985 Geochemistry and petrogenesis of amphibolites, Kolar Schist Belt, South India: evidence for komatiite magma derived by low percentages of melting of the mantle; *J. Petrol.* **26** 92–123
- Schilling J G 1966 Rare earth fractionation in Hawaiian volcanic rocks; *Unpublished Ph.D. Thesis. Mass. Inst. Tech., (USA: Cambridge MA)*
- Singh A K and Vallinayagam G 2002 Geochemistry and petrogenesis of granite in Kundal area, Malani Igneous Suite, Western Rajasthan; *J. Geol. Soc. India* **60** 183–192
- Storey B C, Alabaster T, Hole M J, Pankhurst R J and Wever H E 1992 Role of subduction-plate boundary forces during the initial stages of Gondwana break up: evidence from the proto-pacific-margin of Antarctica; *Geol. Soc. London. Spec. Publ.* **68** 149–164
- Sun S S and McDonough W F 1989 Chemical and isotopic systematic of oceanic basalts: implications for mantle composition and processes, In: *Magmatism in the oceanic basins* (eds) A D Saunders, M J Norry; *Geol. Soc. London Sp. Publ.* **42** 313–345

- Sun S S and Nesbitt R W 1977 Chemical heterogeneity of the Archaean mantle, composition of the bulk earth and mantle evolution; *Earth Planet Sci. Lett* **35** 429–448
- Takahashi E 1986 Melting of dry peridotite KLB1 upto 14 GPa: implications on the origin of peridotite upper mantle; *J. Geophys. Res.* **91** 9367–9382
- Taylor S R and McLennan S M 1985 *The continental crust: Its composition and evolution* (Oxford: BlackWell scientific field) 312
- Torsvik T H, Carter L M, Ashwal L D, Bhushan S K, Pandit M K and Jamtveit B 2001 Rodinia refined or obscured: Palaeomagnetism of the Malani Igneous Suite (NW India); *Precam. Res.* **108** 319–333
- Vallinayagam G 1997 Mineral chemistry of Siwana ring complex; *J. Ind. Mineral.* **31** 37–47
- Vallinayagam G 2001 Geochemistry and petrogenesis of basic rocks in the Siwana ring complex, Barmer district, Rajasthan, India; *J. Ind. Mineral.* **35** 121–133
- Vallinayagam G and Kochhar N 1998 Geochemical characterization and petrogenesis of A-type granites and the associated acid volcanics of the Siwana ring complex, northern Peninsular, India. In: *The Indian Precambrian* (ed) B S Paliwal; (Jodhpur: Scientific Publ.) 460–481